J Mater Sci: Mater Electron **(2025) 36:1468**

Photodiode and photodetector characteristics of Ag/MnPc/Si/Ag and Ag/MnPc/SiO_2/Ag heterojunctions

Fatih Ünal[1,2,*], Mümin Mehmet Koç[3,4,*], Sitki Aktas[5], Burhan Coşkun[3], Mustafa Şükrü Kurt[6,7], Mahmut Gür[8], and Tayfun Arslan[9]

[1] *Central Research Laboratories, Application and Research Centre, GRUMLAB, Giresun University, 28200 Giresun, Türkiye*
[2] *Department of Physics, Faculty of Art and Science, Giresun University, Giresun, Türkiye*
[3] *Department of Physics, Faculty of Art and Science, Kirklareli University, Kirklareli, Türkiye*
[4] *Department of Health Service and Techniques, School of Health Service, Kirklareli University, Kirklareli, Türkiye*
[5] *Department of Mechanical Engineering, Faculty of Engineering, Giresun University, Giresun, Türkiye*
[6] *Department of Fundamental Science, Science Faculty, Erzurum Technical University, Erzurum, Türkiye*
[7] *Department of Physics, Faculty of Engineering and Natural Science, Bursa Technical University, Bursa, Türkiye*
[8] *Department of Forest Industrial Engineering, Faculty of Forestry, Kastamonu University, Kastamonu, Türkiye*
[9] *Department of Chemistry, Faculty of Science, Giresun University, Giresun, Türkiye*

Received: 24 October 2024
Accepted: 11 August 2025
Published online: 19 August 2025

ABSTRACT

Manganese (III) phthalocyanine (4) (modified MnPc) was synthesized by tetramerization of the relevant phthalonitrile under appropriate conditions and thermally coated on Si and SiO_2 coated surfaces for the preparation of Ag/MnPc/Si/Ag and Ag/MnPc/SiO_2/Ag heterojunctions. Series of investigation methods were applied to assess structural, optical and optoelectronic properties. For the assessment of surface morphology and structure, scanning electron microscopy (SEM) and X-ray diffractometry (XRD) techniques were applied, respectively. Optical properties were evaluated using UV–vis spectrophotometry where energy band gap of the MnPc, Si and SiO_2 thin films were derived as 2.46 eV, 2.79 eV and 2.6 eV, respectively. I-V investigation was employed in dark and under various illumination intensities in 20 mW.cm^{-2}, 40 mW.cm^{-2}, 60 mW.cm^{-2}, 80 mW.cm^{-2} and 100 mW.cm^{-2}. Using I-V data different device parameters like ideality factor, serries resistance and barrier height values were derived. Besides various photodetector and photosensitivity parameters were calculated. It was seen that Ag/MnPc/Si/Ag and Ag/MnPc/SiO_2/Ag heterojunctions are sensitive to light but no direct correlation between light intensity and diode parameters were seen.

Address correspondence to E-mail: fatih.unal@giresun.edu.tr; muminmehmetkoc@klu.edu.tr

https://doi.org/10.1007/s10854-025-15575-4

1 Introduction

Nanomaterials in thin film form can be used in wide range of disciplines which leads various technological applications [1]. Such materials can be a solution for various problems in the field of electronic, optronic and photonic. [1]. Various types of materials have been worked in those fields. Generally, metals, metal oxides and organic-based materials have preferred in electronic, optoelectronic and photonic applications [2–6]. Each type of material can have certain pros and cons. For example, metals were found to be durable and resistant to external factors [5]. They have good electrical and electronical properties and low absorption rate in light in visible range [5]. Such a case makes them a suitable candidate for optoelectronic, photovoltaic (PV) and solar harvesting applications [5]. However, they are not preferred in flexible applications since they are stiff and exhibit high hardness [7, 8]. On the other hand, organic-based materials often considered as a suitable material for flexible applications where electrical and electronical properties of such materials were found to be reasonably low. Combination of such organic materials with metal-based compounds evidenced to provide enhanced electrical, optical, electronical and optoelectronic performance [9–12]. The combination of organic compounds with metals such as synthesis or doping of organic compounds with metals results in organometallic structures. Such materials were processed as films, heterostructures and heterojunctions [13]. Since such structures have improved electrical, electronic, and optoelectronic performance organometallic materials are often preferred for the organic light emitting diodes (OLEDs), organic field emission transistors (OFETs), organic photovoltaics (OPVs), photodetectors and sensors [9, 10, 14, 15]. At this point, heterostructures step forward in terms of optoelectronic device architecture since such structure exhibit outstanding performance. Heterostructures are multi-layered thin films consisting of different types of films ordered in a special form [16]. The thing makes these structures unique is interface regions which may have role in the identification and characteristics of the films [16]. Moreover, types of the films also affect the characteristics of such structures where organic, organometallic materials, metals and metal oxides can be preferred for the fabrication process. All the mentioned factors can alter the intrinsic factors of heterostructures such as charge carrying capacity, mobility, electrical and optoelectronic characteristics of the structures. A variety of organic materials were employed in the construction of heterostructures. Among those phthalocyanine becoming more popular due to the stability [17]. Phthalocyanine is a compound which can easily be modified with metals and metal oxides where materials in organometallic structures can be produced with improved electric, optic and optoelectronic properties. Therefore, phthalocyanine-based OFETs, OPVs, photodetectors and solar harvesting devices with high efficiencies were reported in the literature [18, 19]. In addition, phthalocyanine is often doped with different materials such as Cu and Zn to enhance its intrinsic characteristics [13, 20–22]. Hence, we managed to produce Mn doped phthalocyanine and used it as photoactive material in heterostructures to produce heterojunctions in Ag/MnPc/Si/Ag and Ag/MnPc/SiO_2/Ag form. We investigated the surface morphology and structural properties of the heterojunctions using scanning electron microscopy (SEM) and X-ray diffractometry (XRD). We also assessed the optical properties to determine optical band gap of the films. We also assessed the I-V characteristics of devices to derive performance of the heterojunctions where photodiode and photodevice characteristics were implemented. We believe that Ag/MnPc/Si/Ag and Ag/MnPc/SiO_2/Ag heterojunctions have potential to be used in flexible electronic applications. Due to the stability of the MnCp base structure, it may be possible to produce durable and flexible electronic and optoelectronic devices with high efficiency.

2 Materials & methods

For this work, heterojunctions in two different structures (Ag/MnPc/Si/Ag and Ag/MnPc/SiO_2/Ag) were produced. Modified MnPc (manganese (III) phthalocyanine (4)) was produced in accordance with the following method. Modified MnPc (manganese (III) phthalocyanine (4)) was produced by a modified method according to the literature [23]. The cyclotetramerization of (E)-4-(3-(3-(2,4,6-trimethoxyphenyl) acryloyl)phenoxy)phthalonitrile in the presence of anhydrous $MnCl_2$ in n-pentanol (5 mL) and DBU under N_2 gas applied the modified MnPc. This process yielded 0.024 g (24%) of the final product, which had a melting point of over 300 °C. All newly synthesized compounds were confirmed by spectroscopic methods, and it is fully consistent with literature values.

Heterojunctions were fabricated on ITO (indium tin oxide)/glass substrate. Prior to the production, a cleaning procedure was applied to the ITO/glass substrates. For this purpose, ITO/glass was rinsed with acetone and sonicated in propanol in for 5 min. Sonicated ITO/glass substrate then nitrogen blowed.

While fabrication of the Ag/MnPc/Si/Ag and Ag/MnPc/SiO2/Ag heterojunction, the Si (200 nm) and SiO_2 (100 nm) thin film layers were coated on the ITO/glass substrates using the Nanovak NVTS-400 DC magnetron sputtering system at room temperature. Two-inch diameter Si and SiO_2 sputter targets with a purity of 99.99% were utilised. Prior to deposition, both targets underwent a 10-min plasma cleaning process to remove impurities and enhance surface reactivity. During the deposition of the silicon film, the base pressure and process pressure were maintained at approximately 3×10^{-6} Torr and 4×10^{-3} Torr, respectively, with an argon gas pressure of 4 mTorr. The deposition rate was monitored continuously by an XTM (quartz thickness monitor), with a rate of between 0.3 and 0.45 $Å.s^{-1}$ achieved by applying DC power of 540 V / 210 mA. Similarly, the base pressure and process pressure were maintained at approximately 3.2×10^{-6} mTorr and 4.3×10^{-3} mTorr, respectively, with an argon gas pressure of 4 mTorr during the deposition of the SiO_2 thin film. The deposition rate was found to be between 0.32 and 0.48 $Å.s^{-1}$ in the SiO_2 thin film production, with the use of a direct current (DC) power supply of 530 V and 200 mA.

Subsequently, the MnPc (≈15 nm) compound was deposited onto the Si and SiO_2 layers at ambient temperature under a vacuum pressure of 10^{-6} Torr through thermal evaporation, facilitated by a Vaksis (PVD-MT/2M2T) system. Subsequently, silver (Ag) contacts (0.77 mm diameter) were formed on the Si-MnPc and SiO2-MnPc layers using a mask with circular apertures, allowing for basic electrical analysis where final form of heterojunction was obtained. Figure 1 shows the schematic representation of Ag/MnPc/Si/Ag and Ag/MnPc/SiO_2/Ag heterojunctions and the band diagram at equilibrium during electrical conduction.

3 Results

3.1 Morphological, structural and optical characteristics

The surface morphology images obtained by SEM of the MnPc/Si/ITO/glass and MnPc/SiO_2/ ITO/glass

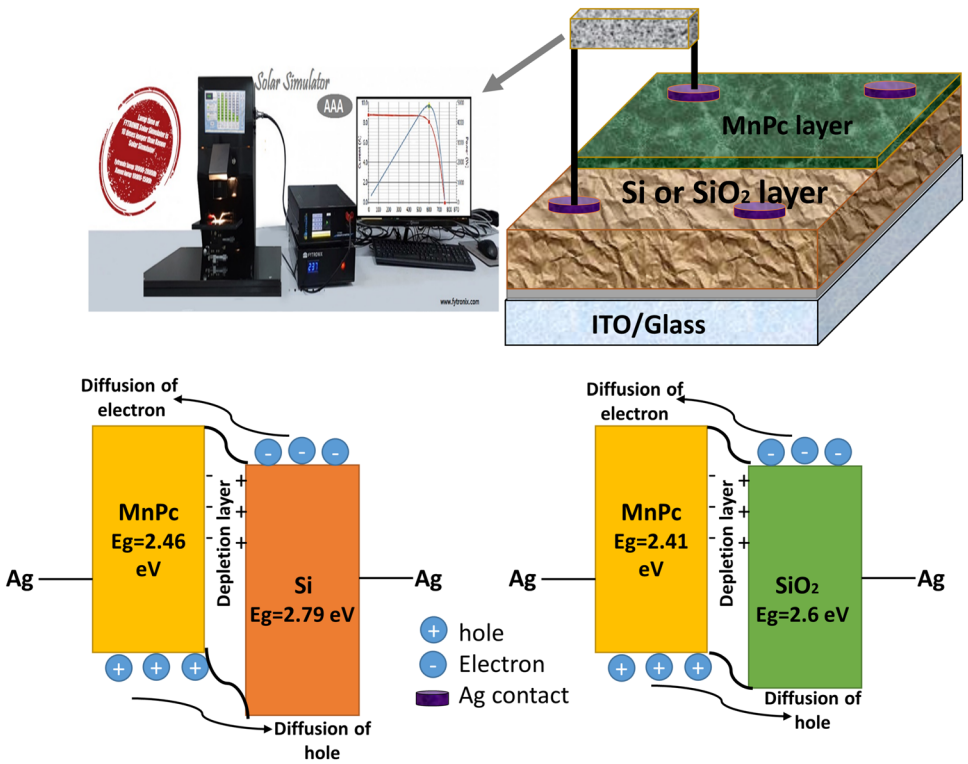

Fig. 1 The schematic representation of Ag/MnPc/Si/Ag and Ag/MnPc/SiO_2/Ag heterojunctions and the band diagram at equilibrium during electrical conduction

heterojunctions are presented in Fig. 2a and 2b, respectively. In Fig. 2a, a smooth surface was seen; couple of lumps around 1 μm can be identified on the surface. Lumps do not affect the smoothness of the surface. In Fig. 2b, grain-like structures can be seen which spread around the surface. The size of the grains was found to be smaller than 1 μm. The surface seems quite smooth.

X-ray diffraction patterns of the Si/ITO/glass and SiO_2/ITO/glass multilayer films are presented in Fig. 3, showing broad distortions and some peaks which are associated with ITO films. Broad noise-like characteristics indicate that no crystallization related formations were achieved. Hence, it can be concluded that Si and SiO_2 structures on ITO films are not in crystal form. No matter what ITO related peaks were identified in both Si/ITO/glass and SiO_2/ITO/glass multilayer films. Therefore, based on XRD, it can be said that both Si and SiO_2 thin films are amorphous in structure.

Using absorbance (A) data (see Fig. 4), the transmittance (T) of MnPc/Si/ITO/glass and MnPc/SiO_2/ITO/glass heterostructures were assessed between the wavelength of 350 nm to 850 nm using the relation between the absorbance and transmittance of A = -logT. Absorbance and transmittance characteristics of the MnPc/Si/ITO/glass and MnPc/SiO_2/ITO/glass heterojunctions obtained using UV–Vis spectroscopy between 350 and 850 nm and are presented in Fig. 4a and Fig. 4b, respectively. Absorbance characteristics of MnPc/Si/ ITO/glass films shows slight decrease with increasing wavelength. MnPc/Si/ITO/glass films show slightly high absorbance rate between 350 and 500 nm such a case indicate that films absorb light in UV zone. Similarly, transmittance rate of the MnPc/Si/ITO/glass films exhibit increasing trend with increasing wavelength. MnPc/SiO_2/ITO/glass films exhibit drastic increase on absorbance between 350 and 400 nm wavelength. After 400 nm, a dramatic

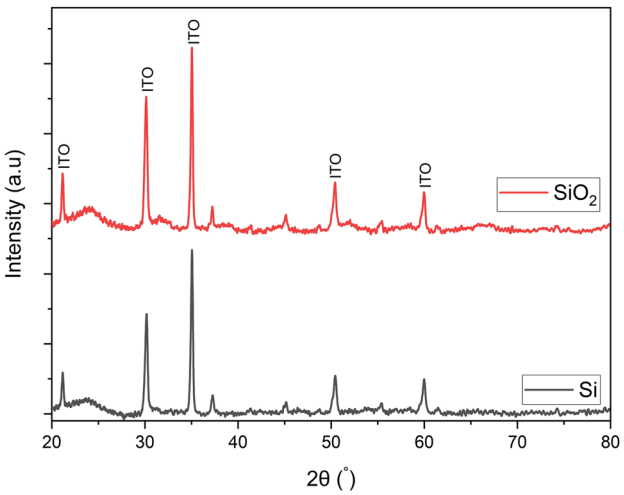

Fig. 3 X-ray diffraction patterns obtained from Si and SiO_2 thin films on the ITO/glass

decrease on absorbance between 400 and 550 nm were observed. A slight peak was observed between 550 and 700 nm. A similar trend was also observed for transmittance for MnPc/SiO_2/ITO/glass thin films. Transmittance of MnPc/SiO_2/ITO/glass films dramatically decrease between 350 and 390 nm. A sharp increase in transmittance between 400 and 550 nm was seen. A small diminishing trend in transmittance was observed between 550 and 700 nm. Another peak between 700 and 850 nm was observed. It was seen that transmittance and value for MnPc/SiO_2/ITO/glass films alters depending on wavelength which indicate that the wavelength alters transmittance characteristics of MnPc/SiO_2/ITO/glass films.

The energy band gap (E_g) is derived employing the Tauc plot method via the equation $(h\nu)\approx(h\nu\text{-}E_g)^m$, related to the absorption coefficient, where m is equal to ½ for direct allowed transition and $h\nu$ is the photon energy [24]. The energy band gap can be determined

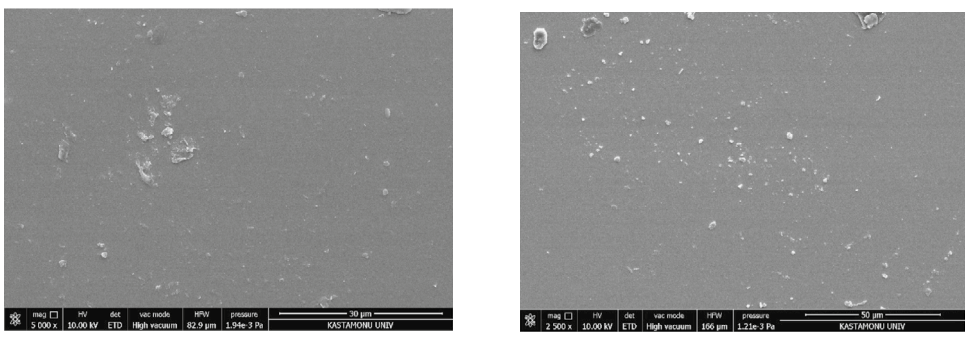

-a- -b-

Fig. 2 Surface SEM images of a) MnPc/Si/ITO/glass and b)MnPc/SiO_2/ITO/glass heterojunctions

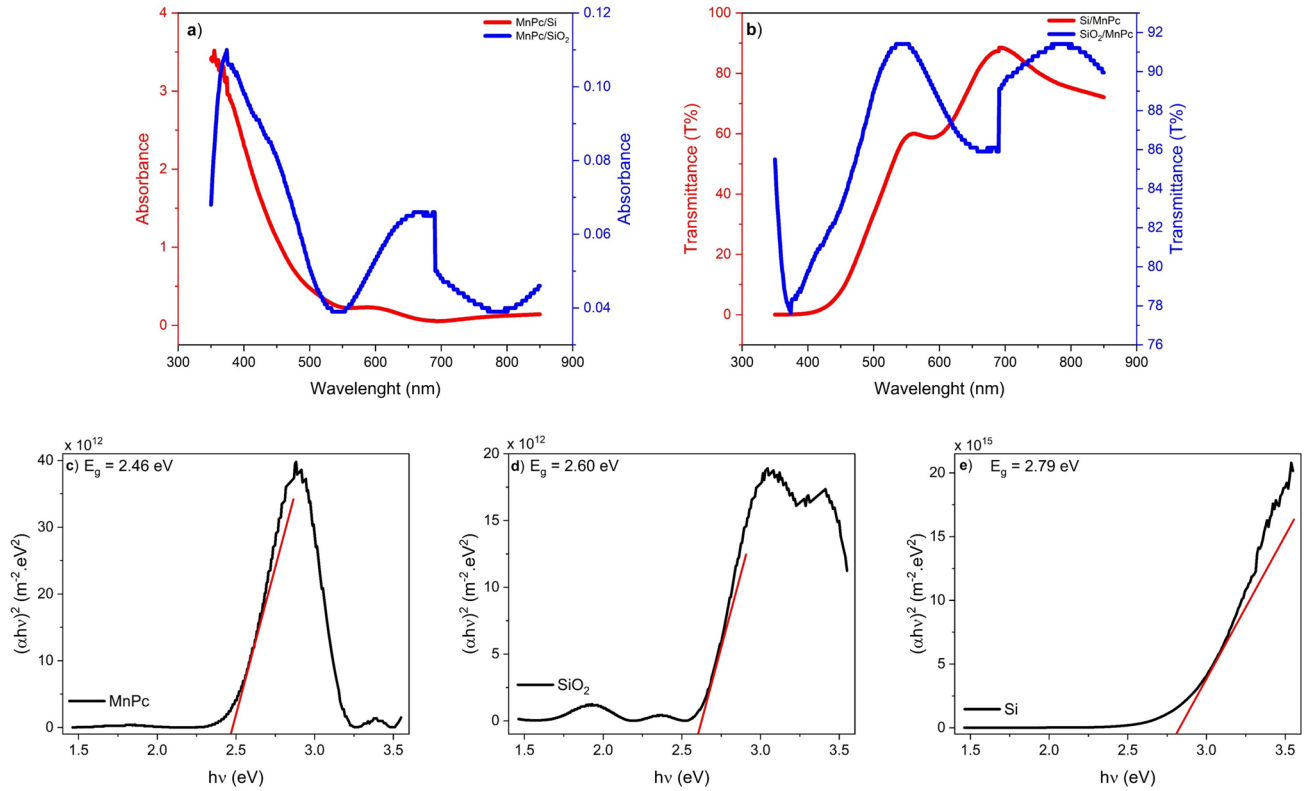

Fig. 4 Absorbance-wavelength heterojunctions **a**, transmittance-wavelength heterojunctions **b**, band gap energies of MnPc **c**, band gap energies of SiO_2 **d** and band gap energies of Si **e** thin films deposited on ITO/glass

by extrapolating the linear portion of $(\alpha hv)^2$ to the photon energy (αhv) axis from a plot of $(\alpha hv)^2$ versus hv. Energy band gap of the MnPc, Si and SiO_2 thin films deposited on ITO/glass substrates were found to be 2.46 eV, 2.79 eV and 2.6 eV, respectively. The energy band gap of the MnPc was found to be lower than the energy band gap for MnPc thin films reported in the literature. For example, Rajesh and Menon determined the E_g of MnPc/Au thin films as 2.88 eV [25]; Qasrawi and Zyoud determined the energy band gap of Mn/ZnPc interfaces as 2.62 eV [21]; Rajesh and Menon found the thickness related E_g of MnPc thin films between 3.14 eV and 3.25 eV [26]; Arshak et al. found the energy band gap of MnPc thin films as 2.59 eV [27]; Günsel et al. determined the energy band gap of MnPc thin films as 2.98 eV [28].

3.2 Photodiode and photodetector characteristics

I-V characteristics of Ag/MnPc/Si/Ag and Ag/MnPc/SiO_2/Ag heterojunctions were obtained between at -1 V and + 1 V applied potential under daylight in varying light intensities. I-V results pertaining the heterojunctions are presented in Fig. 5. It was concluded that heterojunctions are responsive to light. Utilizing I-V data of the different parameters related the photodetector properties were assessed. In the calculations, thermionic emission theory was used.

$$I = AA * T^2 \exp\left(\frac{-q\Phi_B}{kT}\right)\left[\exp\left(\frac{q(V - IR_s)}{kT}\right) - 1\right], \quad (1)$$

where Φ_b is the barrier height, A* is the Richardson constant, k is the Boltzmann constant, T is the Kelvin temperature, q is the charge of the electron, A is the active surface area of the diode, V is the potential, R_s is the serries resistance,

Equation 1 when V-IR_s > > 3kT

$$I = I_0 \exp\left(\frac{qV}{nkT}\right) \quad (2)$$

$$I_0 = AA * T^2 \exp\left(\frac{-q\Phi_B}{kT}\right) \quad (3)$$

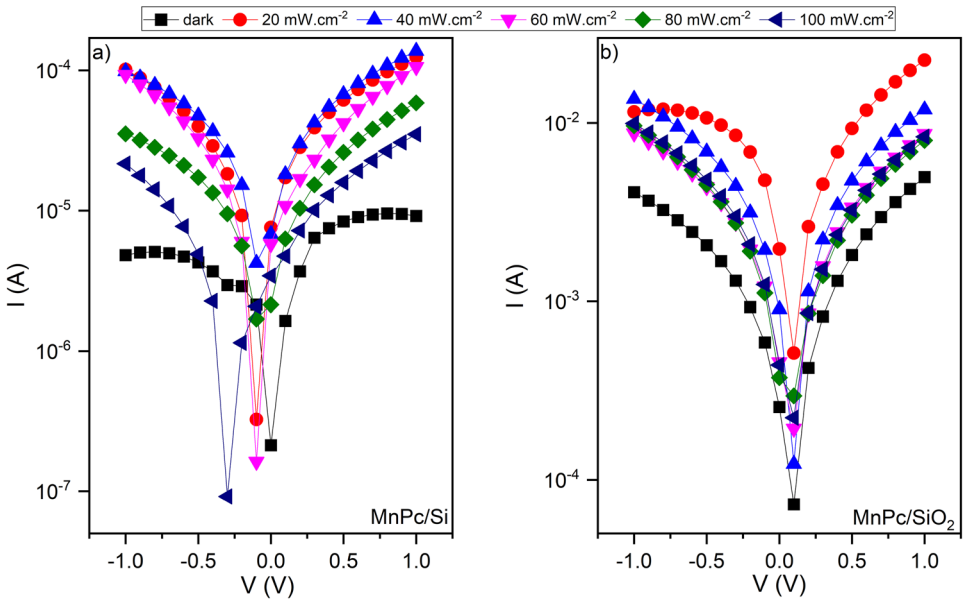

Fig. 5 I-V characteristics of (**a**) Ag/MnPc/Si/Ag and (**b**) Ag/MnPc/SiO_2/Ag heterojunctions

Equation 7 is obtained by taking derivative of V after taking the logarithm of Eq. 2.

$$n = \frac{q}{kT}\frac{d(v}{dd(\ln(I))} \tag{4}$$

ln(I) against V in the low voltage region (the region where the I-V curve is linear) is calculated together with other constants, the ideality factor n is found. The graph of ln(I) against V intersects ln(I) gives reverse saturation current. Here, Eq. 3 gives the barrier height Φ_b.

Light intensity related ideality factor (n), barrier height Φ_b, photocurrent I_0, and series resistance R_s (from Rj = dV/dI) characteristics of Ag/MnPc/Si/Ag and Ag/MnPc/SiO_2/Ag heterojunctions are presented in Fig. 6 and all values are listed in Table 1 and Table 2, respectively.

Ideality factor of Ag/MnPc/Si/Ag heterojunctions were found between 5.68 and 10.25 while ideality factor of Ag/MnPc/SiO_2/Ag heterojunctions were found between 3.18 and 4.04. It was seen that the ideality factor values of Ag/MnPc/SiO_2/Ag heterojunctions deviates less than Ag/MnPc/Si/Ag heterojunctions. It was expected to see an ideality factor a photodiode around 1. However, it is impossible to provide a diode with ideality factor 1. Various parameters affect the ideality factor such as interface states, interlayer oxidations, series resistance effect [29]. Observing the ideality factors bigger than 1 is commonly reported in literature especially for organic-based heterojunctions. For example; Günsel et al. reported the ideality factor of MnPc-based photodiodes as 8.89 [28]; Unal et al. found the ideality factor for H_2Pc/CuO heterojunctions between 10.34 and 14.82 [30]; Aktas et al. found the ideality factor for MnPc heterojunctions as 5.60 [31]; Aktas et al. found the ideality factor for In/WO_x/CuPc/In heterojunctions between 8.70 and 16.83 [13]; Gorunmez Gungor et al. found the ideality factor for Al/p-Si/CuPc/Al structures as 8.18 [32]. Our results were found to be coherent with the results reported in the literature (Fig. 7).

Barrier height of Ag/MnPc/Si/Ag heterojunctions were found between 0.57 eV and 0.64 eV while barrier height of Ag/MnPc/SiO_2/Ag heterojunctions were found between 0.49 eV and 0.55 eV. No direct correlation between illumination intensity and barrier height was seen. Barrier height, and other parameters vary with power of light source. This situation can be explained by the rearrangement and organization of the molecular structures in the layers as the light falls on the layers [33, 34]. Our results indicate that our results are consistent with the results in the literature. For example, Günsel et al. reported the barrier height of MnPc-based photodiodes as 0.91 eV [28]; Unal et al. found the barrier height for H_2Pc/Cu heterojunctions between 0.424 eV and 0.436 eV [30]; Aktas et al. found the barrier height for MnPc/Gc heterojunctions as 0.71 eV [31]; Aktas et al. found the barrier height for In/WO_x/CuPc/In heterojunctions

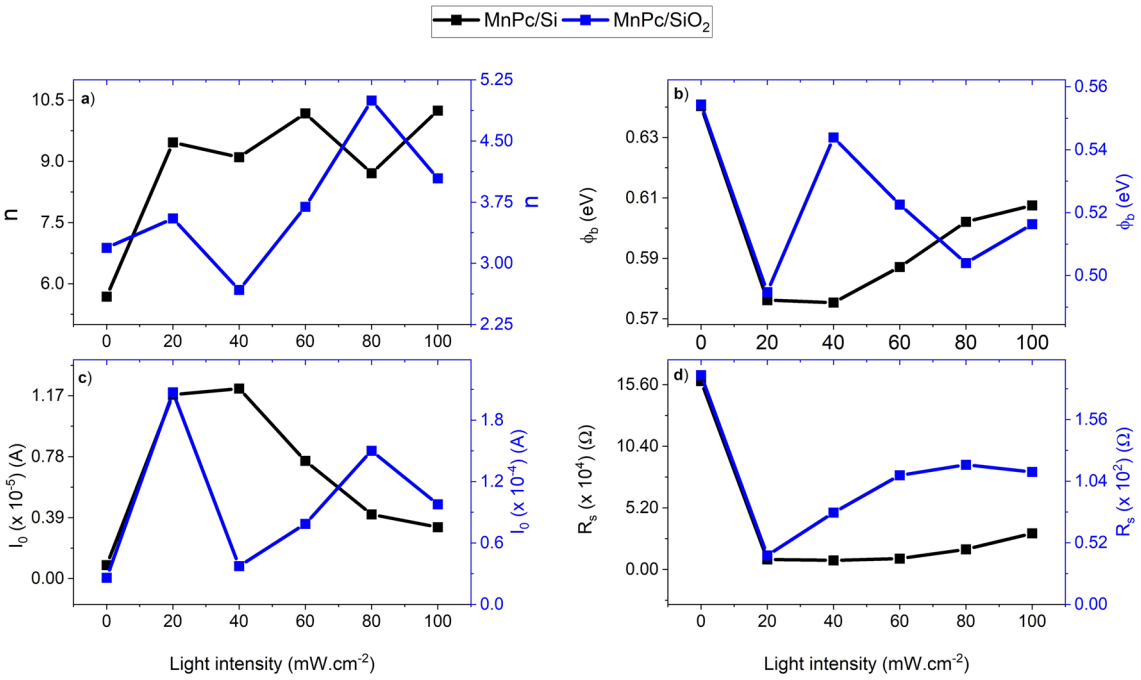

Fig. 6 Light intensity related **a** ideality factor (n), **b** barrier height (Φ_b), **c** reverse saturation current (I_0) and **d** series resistance (R_s) characteristics of Ag/MnPc/Si/Ag and Ag/MnPc/SiO_2/Ag heterojunctions

Table 1 Diode parameters of Ag/MnPc/Si/Ag heterojunctions

Light Intensity (mW/cm^2)	Thermionic Emission Theory			*Ohm's law*
	n	Φ_b *(eV)*	I_o *(A)*	R_s *(Ω)*
0	5.68	0.640	8.66×10^{-7}	159,051.68
20	9.46	0.573	1.17×10^{-5}	8485.14
40	9.10	0.572	1.21×10^{-5}	7584.40
60	10.17	0.584	7.5×10^{-6}	9194.06
80	8.70	0.600	4.10×10^{-6}	17,072.04
100	10.24	0.606	3.28×10^{-6}	30,422.46

Table 2 Diode parameters of Ag/MnPc/SiO_2/Ag heterojunctions

Light Intensity (mW/cm^2)	*Thermionic Emission Theory*			*Ohm's law*
	n	Φ_b *(eV)*	I_o *(A)*	R_s *(Ω)*
0	3.18	0.55	2.60×10^{-5}	193.44
20	3.54	0.49	2.07×10^{-5}	41.34
40	2.67	0.54	3.74×10^{-5}	77.52
60	3.69	0.52	7.86×10^{-5}	109.05
80	4.99	0.50	1.5×10^{-4}	117.80
100	4.04	0.51	9.77×10^{-5}	111.91

between 0.48 eV and 1.20 eV [13]; Gorunmez Gungor et al. found the barrier height for Al/p-Si/CuPc/Al structures as 0.35 eV [32].

Reverse saturation current of Ag/MnPc/Si/Ag heterojunctions were found between 8.66×10^{-7}A and 1.21×10^{-5} A while saturation current of Ag/MnPc/SiO_2/Ag heterojunctions were found between 1.5×10^{-4}A and 2.07×10^{-5} A. A direct relation between saturation current and illumination intensity was not found. It was concluded that the results obtained from our experiments were found to be coherent with the results previously reported. For example, Unal et al. found the saturation current for H_2Pc/CuO heterojunctions between 7.52×10^{-3} A and 1.0×10^{-2} A [30]; Aktas et al. found the saturation current for MnPc/Gc heterojunctions as 1.512×10^{-1} A [31]; Aktas et al. found the saturation current for In/WO_x/CuPc/In heterojunctions between -4.8×10^{-8} A and -1.2×10^{-7} A [13]; Gorunmez Gungor et al. found the saturation current for Al/p-Si/CuPc/Al structures as 0.02815 A [32].

Series resistance of Ag/MnPc/Si/Ag heterojunctions were found between 9.1 kΩ and 159 kΩ while series resistance of Ag/MnPc/SiO_2/Ag heterojunctions were found between 41Ω and 193 Ω. Resistance and illumination values were not found to be directly

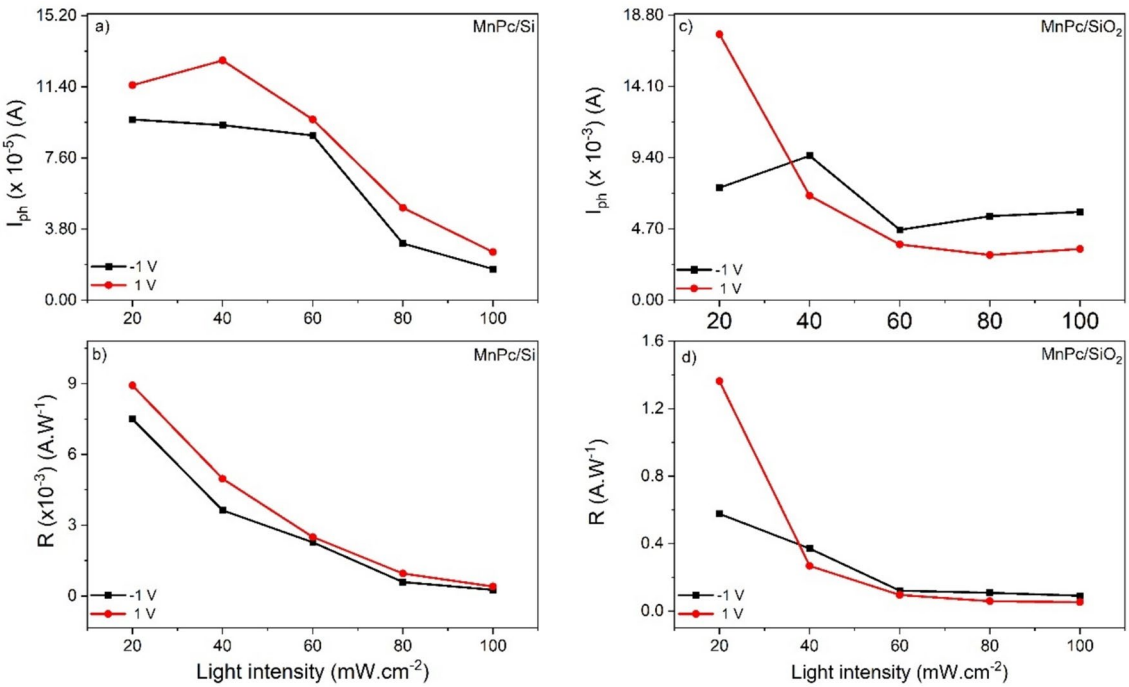

Fig. 7 Light intensity related **a** photocurrent and **c** photoresponsivity values for Ag/MnPc/Si/Ag heterojunction and light intensity related **b** photocurrent and **d** photoresponsivity values for Ag/MnPc/SiO_2/Ag heterojunctions obtained between -1 V and +1 V

related. Results in the literature are as follows which were found to be related to our results. For example, the series resistance of MnPc-based photodiodes was reported as 102.6 kΩ [28]; series resistance for H_2Pc/Cu heterojunctions was found between 13.67 Ω and 17.65 Ω [30]; series resistance for MnPc/Gc heterojunctions was reported as 28 Ω [31]; the series resistance for Al/p-Si/CuPc/Al structures was reported as 5.56 Ω [32].

Photoconductive responsivity (R_{ph}) is an essential indicator which gives an indication about a photodiode responds to incoming light [35, 36]. The parameter can be determined as the ratio of generated photocurrent ($I_{ph} = I_{ill}$-I_{dark}) to the optical power of the incoming light. I_{ill} and I_{dark} are the currents under light and in the dark, respectively. The following equation can be used for the determination of photoconductive responsivity [37–39]:

$$R_{ph} = \frac{I_{ph}}{P_{inc}A^{i}}, \tag{5}$$

where A^i refers to the irradiated active area ($6.44 \times 10^{-5} m^2$), P_{inc} is the intensity of incoming light. R_{ph}, and I_{ph} values of the Ag/MnPc/Si/Ag and Ag/MnPc/SiO_2/Ag heterojunctions obtained at altering light intensities is presented in Table 3 and Table 4. The values were obtained at varying light intensities between 20 mW/cm^2 and 100 mW/cm^2 with a ± 1 V applied potential. Photocurrent values of Ag/MnPc/Si/

Table 3 Photodetector parameters of Ag/MnPc/Si/Ag heterojunctions

Light Intensity (mW/cm^2)	*I_{ph} (A)*		*R_{ph} (A/W)*		*PS%*		*D* (Jones)*	
	-1 V	*1 V*	*-1 V*	*1 V*	*-1 V*	*1 V*	*-1 V*	*1 V*
20	9.66×10^{-5}	1.1×10^{-4}	0.0075	0.0089	1913	1357	4.85×10^{7}	4.18×10^{7}
40	9.35×10^{-5}	1.2×10^{-4}	0.0036	0.0049	1850	1501	2.35×10^{7}	2.33×10^{7}
60	8.81×10^{-5}	9.65×10^{-5}	0.0022	0.0025	1736	1157	1.47×10^{7}	1.17×10^{7}
80	3.03×10^{-5}	4.94×10^{-5}	0.0006	0.0009	533	641	0.38×10^{7}	0.45×10^{7}
100	1.67×10^{-5}	2.57×10^{-5}	0.0003	0.0004	249	381	0.16×10^{7}	0.18×10^{7}

Table 4 Photodetector parameters of Ag/MnPc/SiO_2/Ag heterojunctions

Light Intensity (mW/cm^2)	I_{ph} *(A)*		R_{ph} *(A/W)*		*PS%*		*D* (Jones)*	
	-1 V	*1 V*	*-1 V*	*1 V*	*-1 V*	*1 V*	*-1 V*	*1 V*
20	7.42×10^{-3}	1.75×10^{-2}	0.57	1.36	81	452	12.8×10^{7}	27.4×10^{7}
40	9.54×10^{-3}	6.90×10^{-3}	0.37	0.26	133	238	8.21×10^{7}	5.39×10^{7}
60	4.65×10^{-3}	3.69×10^{-3}	0.12	0.09	13	174	2.67×10^{7}	1.92×10^{7}
80	5.55×10^{-3}	3×10^{-3}	0.11	0.06	35	160	2.38×10^{7}	1.17×10^{7}
100	5.84×10^{-3}	3.39×10^{-3}	0.09	0.05	42	168	2.01×10^{7}	1.06×10^{7}

Ag heterojunction were changed between 1.2×10^{-4}A and 2.57×10^{-5} A, exhibiting decreasing pattern with increasing illumination intensity. Photocurrent values between 1.75×10^{-2} A and 3×10^{-3} A was measured for Ag/MnPc/SiO_2/Ag heterojunctions. Photocurrent decreased with increasing illumination intensity. R_{ph} values for Ag/MnPc/Si/Ag heterojunctions were found to be between 0.05 AW^{-1} and 1.23 AW^{-1}. Diminishing trend was obtained for increasing illumination intensity. R_{ph} values for Ag/MnPc/SiO_2/Ag heterojunctions were found to be between 188.76 AW^{-1} and 7.30 AW^{-1}. Diminishing trend was obtained for increasing illumination intensity.

Table 3 and Table 4 was prepared to sum up the diode parameters for Ag/MnPc/Si/Ag and Ag/MnPc/SiO_2/Ag heterojunctions, respectively. It was seen that I_{ph} values for Ag/MnPc/Si/Ag heterojunctions changes between 9.66×10^{-5} and 1.67×10^{-5} for reverse bias; 1.1×10^{-4} and 2.57×10^{-5} where decreasing trend was obtained for increasing illumination. A slightly different characteristics was observed for Ag/MnPc/SiO_2/Ag heterojunctions where I_{ph} values alter between 9.54×10^{-3} and 4.65×10^{-3} for reverse bias. The maximum I_{ph} value was obtained at 60 mW/cm^2 where minimum I_{ph} value was measured at 40 mW/cm^2. R_{ph} values shows decreasing trend with increasing light intensity in heterojunctions. Such a characteristics is expected observation since enhanced light activates free electrons where reduced resistance value could be observed. PS value exhibit decreasing characteristics with increasing illumination intensity for Ag/MnPc/Si/Ag heterojunctions.

The photosensitivity (PS%) of the Ag/MnPc/Si/Ag and Ag/MnPc/SiO_2/Ag heterojunctions was calculated for -1 V and + 1 V potential range at illumination intensities of 20 mW/cm^2 – 100 mW/cm^2 using the following relation [35, 40, 41]:

$$PS\% = \left(I_{ph} - I_d\right)/I_d x\,100, \tag{6}$$

where I_d is the current in the dark environment. The variation of PS% for Ag/MnPc/Si/Ag and Ag/MnPc/SiO_2/Ag heterojunctions against voltage are illustrated in Fig. 8 (a) and Fig. 8 (b). It can be noted that the PS% under varying illumination intensities obtained with values of 1357.89 (20 mW/cm^2), 1501.70 (40 mW/cm^2), 1157.04 (60 mW/cm^2), 641.30 (80 mW/cm^2), and 381.97 (100 mW/cm^2) for Ag/MnPc/Si/Ag heterojunctions. Similarly, PS% under varying illumination intensities obtained with values of 452.94 (20 mW/cm^2), 238.90 (40 mW/cm^2), 174.30 (60 mW/cm^2), 160.35 (80 mW/cm^2), and 168.31 (100 mW/cm^2) for Ag/MnPc/ SiO_2/Ag heterojunctions. PS% values exhibit decreasing characteristics with increasing light intensity.

Specific detectivity (D*) expresses the low light signal detection capacity of a photodetector. Specific detectivity can be determined utilizing the following equation [42]:

$$D^* = \frac{R_{ph}\sqrt{A^i}}{\left(2qI_d\right)^{1/2}}, \tag{7}$$

where, q is the electron charge. The graph Fig. 8 (c) and Fig. 8 (d) illustrate the calculated D* values versus applied voltage for Ag/MnPc/Si/Ag and Ag/MnPc/SiO_2/Ag heterojunctions. Specific detectivity for Ag/MnPc/Si/Ag heterojunctions were found to be 7.22×10^{11} J (20 mW/cm^2), 4.02×10^{11} J (40 mW/cm^2), 2.02×10^{11} J (60 mW/cm^2), 7.77×10^{10} J (80 mW/cm^2), and 3.24×10^{10} J (100 mW/cm^2). The highest value was obtained for Ag/MnPc/SiO_2/Ag heterojunctions as 4.73×10^{12} J (20 mW/cm^2) while 9.310×10^{11} J (40 mW/cm^2), 3.32×10^{11} J (60 mW/cm^2), 2.02×10^{11} J (80 mW/cm^2), and 1.83×10^{11} J (100 mW/cm^2) for various

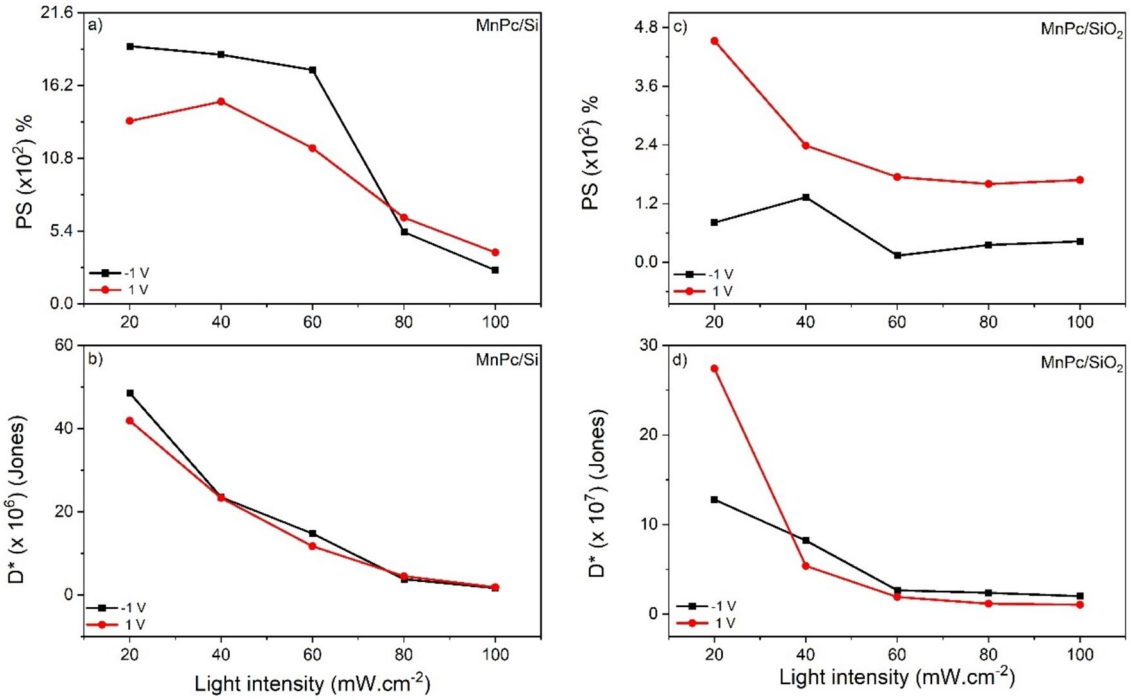

Fig. 8 Light intensity related **a** photosensitivity (PS) and **c** specific detectivity values for Ag/MnPc/Si/Ag heterojunctions and light intensity related **b** photosensitivity (PS) and **d** specific detectivity values for Ag/MnPc/SiO_2/Ag heterojunctions obtained between -1 V and +1 V

illumination intensities. It was noted that D* values were obtained at an illumination intensity of 20 mW/cm^2 while decreasing specific detectivity was obtained for increasing illumination intensity.

4 Conclusion

Optical, optoelectronic and electronic properties of Ag/MnPc/Si/Ag and Ag/MnPc/SiO_2/Ag heterojunctions were assessed. It was concluded that Ag/MnPc/Si/Ag and Ag/MnPc/SiO_2/Ag heterojunctions are sensitive to light. Certain diode characteristics exhibit illuminationn-related behaviour for Ag/MnPc/Si/Ag heterojunctions such as Iph, PS and D*. Same trend was not observed for Ag/MnPc/SiO_2/Ag where some maximum and some minimum values for such characteristics were not obtained in minimum and maximum illumination intensities. Such alterations were attributed to the intrinsic characteristic of heterojunction. On the other hand, no direct correlation was observed for barrier height, ideality factor and series resistance value. It is concluded that intrinsic characteristics of the diodes affects the diode parameters. However, diodes were found to be responsive for light in various illumination intensities. Therefore, they have potential to be used in detector-based applications.

Acknowledgements

The project was supported by Kirklareli University Scientific Research Projects Coordination Office (KLUBAPKO) with reference number of KLUBAP 273. Part of this research was conducted using the facilities of Kırklareli University Advanced Technologies Application and Research Center (ITUAM).

Author contributions

All authors contributed to the study conception and design. FU: drafting, coating of organic thin films and generation of heterojunctions, electrical analysis; MMK: I–V measurement, writing and editing, conceptualisation, formal analysis and writing; SA: writing, editing, design and optical analysis; BC: I–V measurement and writing; MSK: production of Si and

SiO_2 thin film, writing and editing; MG: EDX, SEM and XRD measurement and writing; TA: synthesis of MnPc and writing. All authors read and approved the final manuscript.

Funding

Kırklareli Üniversitesi,KLUBAP 273,Mumin Mehmet Koc

Data availability

The date used in the manuscript can be provided upon a reasonable request.

Declarations

Conflict of interest The authors have no conflicts of interest to declare. All coauthors have seen and agree with the contents of the manuscript and there is no financial interest to report. We certify that the submission is original work and is not under review at any other publication. We declare that we fully accept the rules and policy of the journal.

References

1. J. Jeevanandam, A. Barhoum, Y.S. Chan, A. Dufresne, M.K. Danquah, Beilstein J. Nanotechnol. **9**, 1050 (2018)
2. G. Bräuer, B. Szyszka, M. Vergöhl, R. Bandorf, Vacuum **84**, 1354 (2010)
3. X. Wang, Y. Liao, D. Zhang, T. Wen, Z. Zhong, J. Mater. Sci. Technol. **34**, 1259 (2018)
4. S. Zhang, D. Zhao, *Aerospace Materials Handbook*, 1st edn. (CRC Press, Florida, 2013)
5. X. Yu, T.J. Marks, A. Facchetti, Nat. Mater. **15**(4), 383–396 (2016)
6. S. Bulat, E. Büyükbicakci, M. Erkovan, Energies **17**(2), 430 (2024)
7. H. Ling, S. Liu, Z. Zheng, F. Yan, H.F. Ling, S.H. Liu, F. Yan, Z.J. Zheng, Small Methods **2**, 1800070 (2018)
8. X. Chen, J.A. Rogers, S.P. Lacour, W. Hu, D.H. Kim, Chem. Soc. Rev. **48**, 1431 (2019)
9. W.Y. Wong, C.L. Ho, Acc. Chem. Res. **43**, 1246 (2010)
10. C.L. Ho, H. Li, W.Y. Wong, J. Organomet. Chem. **751**, 261 (2014)
11. J. Lin, D. Ma, Org. Electron. **10**, 275 (2009)
12. M.G. Varnamkhasti, E. Shahriaria, J. Eur. Opt. Soc.-Rapid Publications **10**, 15028 (2015)
13. S. Aktas, F. Unal, M.S. Kurt, M.M. Koç, T. Arslan, M. Gür, B. Coşkun, Z.G. Güngör, Opt. Mater. **138**, 113709 (2023)
14. F. Yakuphanoglu, M.E. Aydin, T. Kiliçoğlu, J. Phys. Chem. B **110**, 9782 (2006)
15. F. Aslan, H. Esen, F. Yakuphanoglu, J. Alloys Compd. **789**, 595 (2019)
16. J.T. Calow, P.J. Deasley, S.J.T. Owen, P.W. Webb, J. Mater. Sci. **2**, 88 (1967)
17. O.A. Melville, B.H. Lessard, T.P. Bender, ACS Appl. Mater. Interfaces **7**, 13105 (2015)
18. R.R. Cranston, B.H. Lessard, RSC Adv. **11**, 21716 (2021)
19. C.G. Claessens, U. Hahn, T. Torres, Chem. Rec. **8**, 75 (2008)
20. S. Varghese, M. Iype, E.J. Mathew, C.S. Menon, Mater. Lett. **56**, 1078 (2002)
21. A.F. Qasrawi, H.M. Zyoud, Physica Status Solidi (b) **257**, 2000089 (2020)
22. Ç. Oruç, A. Erkol, A. Altındal, Anadolu Univ. J. Sci. Technol A – Appl. Sci. Eng. **17**, 717 (2016)
23. T. Arslan, J. Organomet. Chem. **951**, 122021 (2021)
24. N. Dwivedi, S. Kumar, J.D. Carey, R.K. Tripathi, H.K. Malik, M.K. Dalai, ACS Appl. Mater. Interfaces **5**, 2725 (2013)
25. K.R. Rajesh, C.S. Menon, Eur. Phys. J. B-Condens. Matter Complex Syst. **47**(2), 171–176 (2005)
26. K.R. Rajesh, C.S. Menon, Mater. Lett. **51**, 266 (2001)
27. A. Arshak, S. Zleetni, K. Arshak, Sensors **2**(5), 174–184 (2002)
28. A. Günsel, M. Kandaz, F. Yakuphanoglu, W.A. Farooq, Synth. Met. **161**, 1477 (2011)
29. M. Çakar, A. Türüt, Synth. Met. **138**, 549 (2003)
30. F. Unal, S. Aktas, M. S. Kurt, M. M. Koc, T. Arslan, B. Coskun, and M. Gur, J Mater Res 1 (2023).
31. S. Aktas, F. Unal, M.S. Kurt, M.M. Koç, T. Arslan, N. Aslan, B. Coşkun, Phys. Scr. **98**, 095504 (2023)
32. Z.G. Güngör, B. Coşkun, M. İlhan, M.M. Koç, Kırklareli Üniversitesi Mühendislik ve Fen Bilimleri Dergisi **9**, 36 (2023)
33. K.M.A. Saron, M.R. Hashim, N. Naderi, N.K. Allam, Sol. Energy **98**, 485 (2013)
34. Z. Xu, L. Zhang, H. He, J. Wang, M. Xie, J. Appl. Phys. (2011). https://doi.org/10.1063/1.3658850
35. C.A. Canbay, O. Karaduman, J. Mol. Struct. **1235**, 130263 (2021)
36. F. Sarcan, U. Doğan, A. Althumali, H.B. Vasili, L. Lari, A. Kerrigan, F. Kuruoğlu, V.K. Lazarov, A. Erol, J. Alloys Compd. **934**, 167806 (2023)

37. F. Unal, S. Aktas, M.S. Kurt, M.M. Koc, B. Coskun, N. Aslan, T. Arslan, M. Gur, Phys. B Condens. Matter **695**, 416584 (2024)
38. S. Aktas, Opt Mater (Amst) **132**, 112839 (2022)
39. F. Unal, S. Aktas, M.S. Kurt, M.M. Koc, T. Arslan, B. Coskun, M. Gur, J. Mater. Res. **39**, 675 (2024)
40. V. Balasubramani, J. Chandrasekaran, T.D. Nguyen, S. Maruthamuthu, R. Marnadu, P. Vivek, S. Sugarthi, Sens. Actuators A Phys. **315**, 112333 (2020)
41. P. Vivek, J. Chandrasekaran, R. Marnadu, S. Maruthamuthu, J. Electron. Mater. **49**, 4249 (2020)
42. B. Murali, S.B. Krupanidhi, Dalton Trans. **43**, 1974 (2013)